CONTRAST MEDIA & MOLECULAR IMAGING
Contrast Med. Mol. Imaging **1**: 128–137 (2006)
Published online in Wiley InterScience (www.interscience.wiley.com) DOI:10.1002/cmmi.100

CONTRAST MEDIA & MOLECULAR IMAGING

Full Paper

Comparative study of the physicochemical properties of six clinical low molecular weight gadolinium contrast agents†

*Sophie Laurent, Luce Vander Elst and Robert N. Muller**

Department of General, Organic and Biomedical Chemistry, NMR and Molecular Imaging Laboratory, University of Mons-Hainaut, 24 Avenue du Champ de Mars, B-7000 Mons Belgium

Received 13 February 2006; Revised 22 April 2006; Accepted 27 April 2006

ABSTRACT: This paper compares the physicochemical properties of six low molecular weight clinical complexes of gadolinium studied under identical experimental conditions. Magnevist®, Dotarem®, Omniscan®, ProHance®, MultiHance® and Gadovist® were investigated by oxygen-17 relaxometry at different temperatures and by proton relaxometry at various magnetic fields, temperatures and media [pure water, zinc(II)-containing aqueous solutions and HSA-containing solutions]. Osmolality, viscosity and stability versus transmetallation by zinc(II) ions were added for a more comprehensive description. The relaxivities of the clinical formulations as measured in water are similar in the imaging magnetic field region, with a slightly better performance for MultiHance. This can be explained by a shorter distance between the hydrogen nuclei of the water molecule bound to the Gd^{3+} ion and this paramagnetic centre. In contrast to the open-chain complexes, all macrocyclic systems (Dotarem, ProHance and Gadovist) are insensitive to transmetallation by zinc ions. The stability of the open-chain complexes with respect to transmetallation depends on the chemical structure of the ligand, with a better stability for MultiHance. The presence of human serum albumin has no significant effect on the proton relaxivity of Magnevist, Dotarem, Omniscan, ProHance and Gadovist but markedly increases the relaxivity of MultiHance because of a non-covalent interaction with the protein. As a result, the relaxivity of MultiHance in HSA-containing media of fixed concentration decreases with increasing concentration of the contrast agent. Copyright © 2006 John Wiley & Sons, Ltd.

KEYWORDS: MRI contrast agents; proton relaxometry; water residence time; stability

INTRODUCTION

The use of gadolinium paramagnetic complexes as contrast agents to improve the diagnostic capability of magnetic resonance imaging (MRI) has been the subject of numerous studies (1,2). The open-chain Gd–DTPA (gadopentetate dimeglumine, Magnevist®; Schering, Berlin, Germany) and the macrocyclic Gd–DOTA (gadoterate meglumine, Dotarem®; Guerbet, Aulnay-sous-Bois, France) (Fig. 1) were the first representatives of a new generation of these imaging agents. Such complexes are characterized by low toxicity, high thermodynamic and kinetic stabilities, rapid renal clearance, an extracellular biodistribution and a low specificity. Although this concept is of lesser impact in MRI, the clinical formulations of these two complexes present a relatively high osmolality (3–6). Two neutral non-ionic gadolinium chelates, Gd–DTPA–BMA (7) (gadodiamide, Omniscan®; Nycomed, Oslo, Norway) and Gd–HP–DO3A (8) (Gadoteridol, ProHance®; Bracco, Milan, Italy) (Fig. 1), with chemical structures closely related to the two parent compounds but showing lower osmolalities, were subsequently developed and commercialised. More recently, another macrocyclic neutral paramagnetic complex, Gd–DO3A–butrol (gadovist, Gadobutrol®; Schering, Berlin, Germany) (Fig. 1), has been proposed as an extracellular contrast agent (9–11). Since the detection of metastatic focal liver disease is a key health strategy, efforts have also been devoted to produce hepatobiliary contrast agents for MRI. Gd–BOPTA (gadobenate dimeglumine, MultiHance®; Bracco, Milan, Italy) (Fig. 1), an ionic derivative of Gd–DTPA, is the prototype of these second-generation contrast agents (12).

The thermodynamic stability constant of all these gadolinium complexes, except for Omniscan, is very large ($K > 10^{20}\,M^{-1}$), but their conditional constants at pH 7.4 are lower and range between 10^{15} and $10^{19}\,M^{-1}$. The osmolality

**Correspondence to*: R. N. Muller, Department of General, Organic and Biomedical Chemistry, NMR and Molecular Imaging Laboratory, University of Mons-Hainaut, 24 Avenue du Champ de Mars, B-7000 Mons Belgium.
E-mail: robert.muller@umh.ac.be
†This article was produced solely by a review of previously published articles in the public domain. The work did not involve patient or other studies requiring ethical approval.
Contract/grant sponsor: FNRS.
Contract/grant sponsor: French Community of Belgium; *contract/grant number:* ARC 00/05-258.

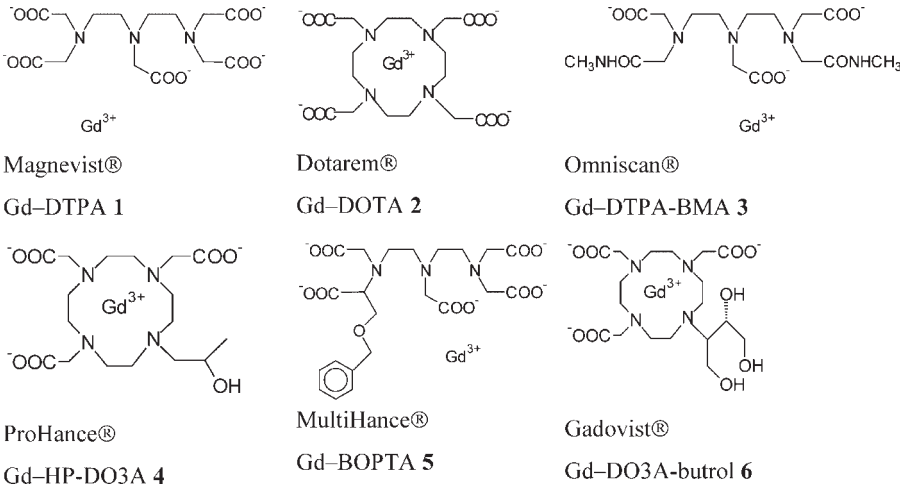

Figure 1. Structures of the contrast agents **1**–**6**.

data and the viscosity values of the commercial formulations are summarized in Table 1 (9,12–15).

In this paper, we report additional physicochemical properties of these six commercially available products, including the water residence time of the coordinated water molecule obtained by oxygen-17 relaxometry since this parameter might have a critical influence on the proton relaxivity of derived structures used as vectorised reporters in molecular imaging. Also reported and interpreted are the proton NMRD profiles at 310 K, the relative stability versus transmetallation process by zinc(II) ions and the possible interaction with serum albumin as evaluated by proton relaxometry.

RESULTS AND DISCUSSION

Proton and oxygen-17 relaxometry

Influence of temperature. It is well established that the residence time of coordinated water molecules (τ_M), a key factor of the relaxivity, can be estimated through the analysis of the temperature dependence of the transverse relaxation rate of the oxygen-17 resonance of bulk water in the gadolinium complex solutions (16–21). The evolutions of the bulk water transverse relaxation rate of oxygen-17 of Gd complexes **1**, **2, 4, 5** and **6** versus temperature are very similar, with the maximum of the reduced transverse paramagnetic relaxation rate at temperatures ranging from 305 to 315 K (Fig. 2), whereas for **3** (Omniscan) the maximum of the experimental data is obtained at a higher temperature (~330 K).

The theoretical adjustment of the experimental data was performed as described previously (16–18). The following parameters were determined: $A/\hbar$, the hyperfine coupling constant between the oxygen nucleus of the bound water molecule and the Gd^{3+} ion; τ_V, the correlation time modulating the electronic relaxation of Gd^{3+}; E_v, the activation energy related to τ_V; B, related to the mean-square of the zero field splitting energy Δ ($B = 2.4\Delta^2$); and $\Delta H^{\neq}$ and $\Delta S^{\neq}$ the enthalpy and entropy of activation, respectively, of the water exchange process. The number of coordinated water molecules was set to one. The calculated parameters are shown in Table 2.

The calculated value of the water residence time at 310 K ranges from 100 to 220 ns for all complexes, except

Table 1. Osmolality, viscosity, thermodynamic and conditional stability constants of the six contrast agents

Complex	Thermodynamic stability constant (log$K$, $\mu = 0.1$)	Conditional stability constant (logK', pH 7.4)	Osmolality[a] (Os kg^{-1} H_2O) (310 K, 500 mM)	Viscosity[a] (mPa s)
Magnevist (**1**)	22.1[b] (298 K)	17.7[c]	1.98[f]	2.90[d]
Dotarem (**2**)	25.4[b] (298 K)	19.0[c]	1.40[f]	2.0[d]
Omniscan (**3**)	16.8[c] (298 K)	14.9[c]	0.645[f]	1.4[d]
ProHance (**4**)	22.8[b] (298 K)	16.9[b]	0.63[d]	1.3[d]
MultiHance (**5**)	22.6[e] (293 K)	18.4[e]	1.97[d]	5.4[d]
Gadovist (**6**)	21.8[d] (298 K)		1.6[d]	4.96[d]

[a]All complex concentrations are equal to 500 mM except for Gadovist (1 M).
[b]From Ref. 13.
[c]From Ref. 14.
[d]From Ref. 9.
[e]From Ref. 12.
[f]From Ref. 15.

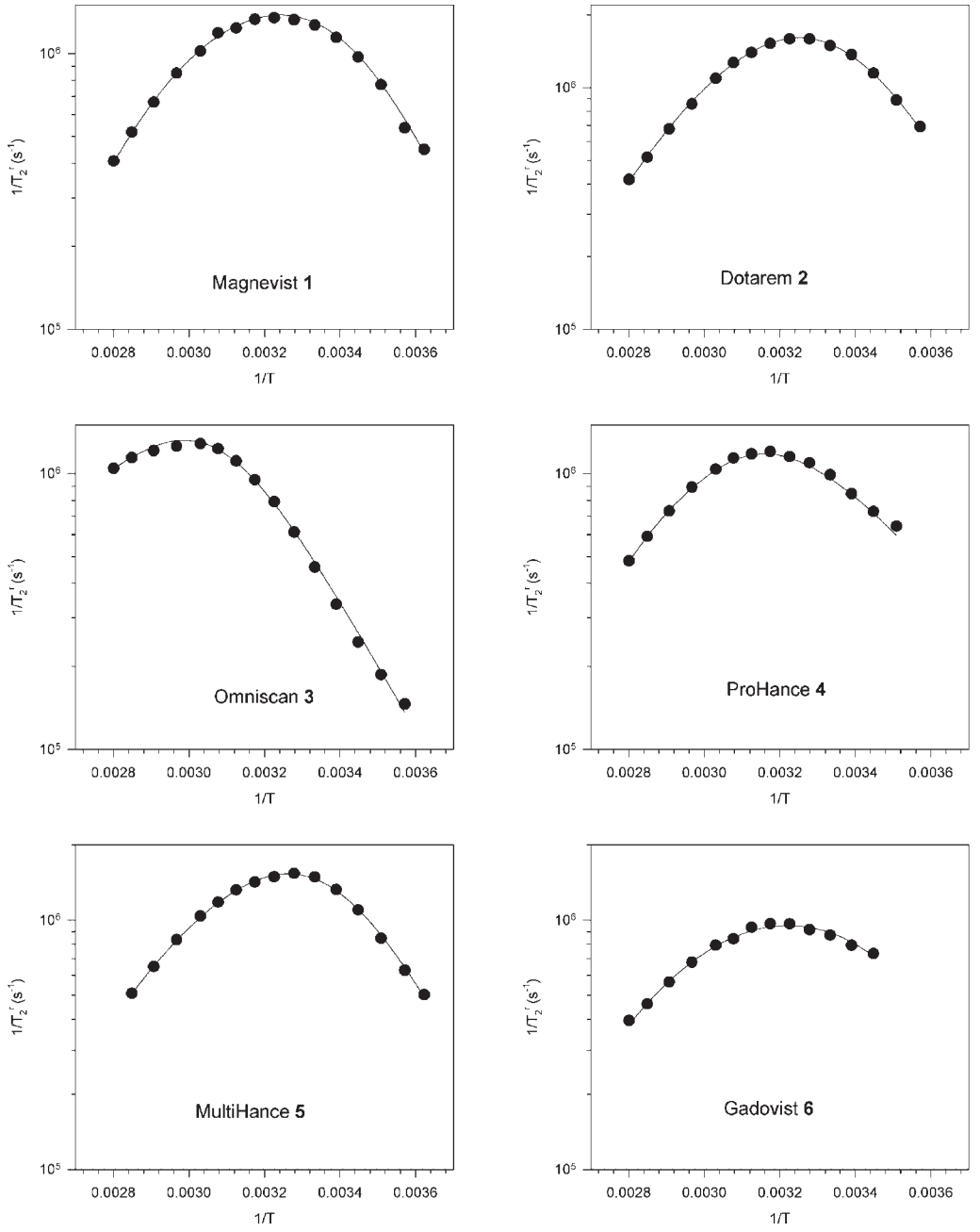

Figure 2. Temperature dependence of the reduced transverse relaxation rate of oxygen-17 at 7.05 T [Magnevist (**1**) from Ref. 18, Omniscan (**3**) from Ref. 23].

for complex **3** which is characterized by a much larger value of τ_M. This phenomenon has already been reported for various bisamide derivatives of Gd–DTPA (19,21–23) and for monoamide and pentamide derivatives of Gd–DTPA (2,24). In the context of the design of tracers for molecular imaging, this behaviour does not favour such a type of covalent coupling of the chelate to its vector. It should also be noted that the τ_M values of all contrast agents studied in this work and more particularly Omniscan **(3)** are not optimum for vectorisation.

The evolution of the longitudinal proton relaxivity versus temperature is known to depend on the residence time of the water molecules coordinated to the Gd(III) ion. When the water exchange is fast over the whole temperature range investigated, the relaxivity increases when temperature is lowered whereas a plateau or a decrease of r_1 is observed when the water residence time becomes a limiting factor. The temperature dependence of the longitudinal proton relaxivity of complexes **1**, **2**, **4**, **5** and **6** confirms that their relaxivity is not limited by their water residence time at low temperatures (Fig. 3). In contrast, and as expected from its slower water exchange rate, the relaxivity of Omniscan (**3**) is limited by the coordinated water residence time at low temperatures.

Table 2. Parameters obtained by the theoretical adjustment of the ^{17}O experimental data

Complex	τ_M^{310} (ns)	$\Delta H^{\neq}$ (kJ mol^{-1})	$\Delta S^{\neq}$ (J mol^{-1} K^{-1})	$A/\hbar$ (10^6 rad s^{-1})	B (10^{20} s^{-2})	τ_v^{298} (ps)	E_v (kJ mol^{-1})
1	143 ± 25[a]	51.5 ± 0.3	52.1 ± 0.6	-3.4 ± 0.1	2.60 ± 0.06	12.3 ± 0.3	4.5 ± 4.2
	~ 130[b]	51.6 ± 1.4	52.0 ± 4.7	-3.8 ± 0.2	1.15 ± 0.05	25 ± 1	1.6 ± 1.8
2	122 ± 10[d]	50.1 ± 0.2	48.7 ± 0.2	-3.42 ± 0.03	1.94 ± 0.09	11.4 ± 0.5	4.0 ± 4.4
	~ 110[b]	49.8 ± 1.5	48.5 ± 4.9	-3.7 ± 0.2	0.38 ± 0.02	11.0 ± 1.0	1.0[e]
3	967 ± 36[c]	48.0 ± 0.1	24.9 ± 0.2	-3.16 ± 0.04	2.04 ± 0.06	21.2 ± 0.6	15.0 ± 11
	~ 1025[b]	47.6 ± 1.1	22.9 ± 3.6	-3.8 ± 0.2	0.99 ± 0.05	25 ± 1	3.9 ± 1.4
4	217 ± 13[d]	49.3 ± 0.1	41.6 ± 0.3	-2.9 ± 0.02	1.55 ± 0.04	8.5 ± 0.2	0.9 ± 10.3
5	140 ± 11[d]	51.1 ± 0.14	51.0 ± 0.2	-3.59 ± 0.56	3.89 ± 0.19	21.3 ± 1.0	12.4 ± 1.7
6	176 ± 21[d]	47.4 ± 0.1	37.2 ± 0.5	-2.80 ± 0.4	1.56 ± 0.04	6.5 ± 0.2	0.9 ± 0.1

[a]From Ref. 18.
[b]From Ref. 22.
[c]From Ref. 23.
[d]This work.
[e]Fixed parameter.

This, however, has no impact on the relaxivity of the compound at physiological temperatures.

Proton NMRD at 310 K. The proton NMRD profiles of complexes **1**, **2**, **3** and **4** at 310 K have already been published (18,25,26). For complex **5**, data obtained at 298 K have been reported (12). Figure 4 shows the data obtained for all complexes at 310 K. The three macrocyclic complexes have the same relaxivity at high magnetic field but, as already reported, Dotarem is characterized by a larger low-field relaxivity, demonstrating a longer electronic relaxation time at zero field (τ_{SO}). The NMRD profiles of the open-chain complexes **1** and **3** are similar whereas the relaxivity of complex **5** is larger over the whole magnetic field range.

The theoretical adjustment of the NMRD profiles takes into account the inner-sphere (27,28) and the outer-sphere (29) contributions to the paramagnetic relaxation rate. Some parameters were fixed during the fitting procedure: q, the number of coordinated water molecules ($q = 1$), d, the distance of closest approach ($d = 0.36$ nm), D, the relative diffusion constant ($D = 3.3 \times 10^{-9}$ m^2 s^{-1}) (26),

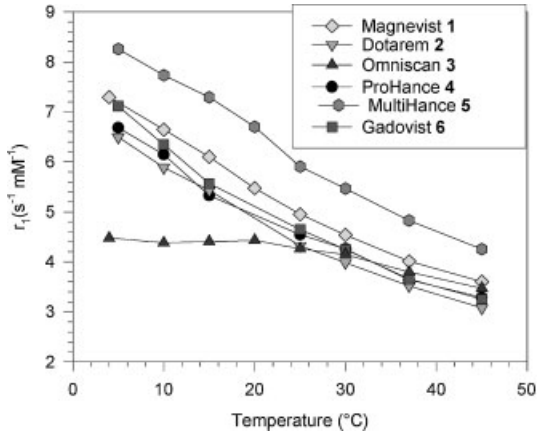

Figure 3. Temperature effect on the proton relaxivity of Gd complexes **1**–**6** at 0.47 T.

and r, the distance between the Gd(III) ion and the proton nuclei of water ($r = 0.31$ nm). The water residence time, τ_M^{310}, was also set to the value determined by ^{17}O NMR. The results of these fittings are shown in Table 3 and Fig. 4. The parameters obtained for complexes **1** and **3** are similar except for the value of τ_M, which is larger for complex **3**. However, as mentioned above, this has no effect on r_1 at 310 K. At lower temperatures, however, its increase clearly limits the relaxivity of Omniscan, as shown in Fig. 2. Performing the theoretical adjustment of the MultiHance (**5**) profile with a distance $r = 0.31$ nm leads to a value of τ_R much larger than expected (dashed line in Fig. 4) and, as already reported by Uggeri *et al.* (12), a more realistic value involves a reduction of the distance between Gd^{3+} and the coordinated water hydrogens. A value of 0.3 nm was chosen based on the data of Caravan et al. (30), who reported that the Gd–H distance of this complex is in the range between 0.30 and 0.32 nm. A decrease in r has also been observed for C4-substituted derivatives of Gd–DTPA (16–18,23). A possible aggregation of the aromatic rings of **5** seems to be unrealistic since, on the one hand, the concentrations used for the proton relaxation measurements are low (≤ 1 mM) and, on the other, deuterium NMR data obtained on higher concentrations of similar complexes (23), do not show evidence of larger τ_R values. For the three macrocyclic derivatives, similar parameters are obtained, except the τ_{SO} value which is much larger for Dotarem **(2)** and is related to the higher symmetry and/or rigidity of this complex.

The corresponding B values calculated from the fit of the proton NMRD data (0.9×10^{20} s^{-1} for **1**, 0.7×10^{20} s^{-1} for **2**, 1.2×10^{20} s^{-1} for **3**, 1.9×10^{20} s^{-1} for **4**, $(0.7–1.1) \times 10^{20}$ s^{-1} for **5** and 2.8×10^{20} s^{-1} for **6**) are different from those obtained from the O-17 data. This may be related to the experimental conditions used in both methods. O-17 data are obtained at high magnetic field where τ_{S1} values are large (of the order of 10^{-8} s) whereas the proton relaxometric NMRD data of small

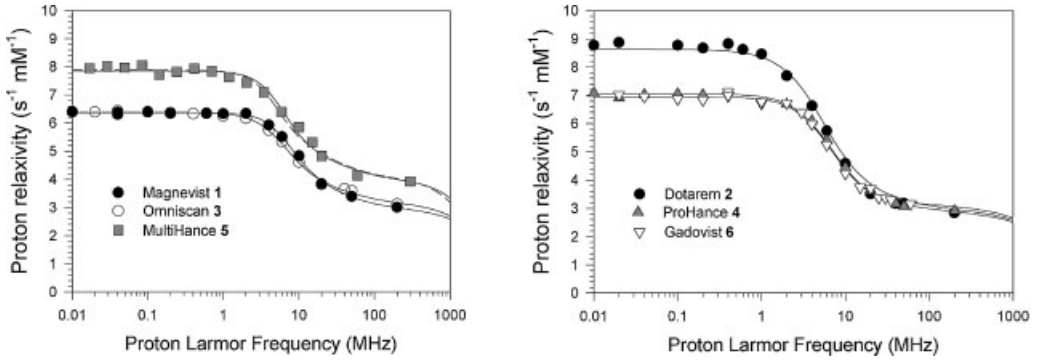

Figure 4. ^{1}H NMRD relaxivity profiles of Gd complexes **1**–**6** in water at 310 K. The lines correspond to the theoretical fittings of the data points.

complexes depend on the electronic parameters mainly at low fields (where τ_{S1} values are of the order of 10^{-10} s) but not at high fields.

Transmetallation

Possible transmetallation by zinc(II) ions was used as a stability test for the six complexes. The procedure takes advantage of the very low solubility of Gd^{3+} ions in phosphate solution and of the subsequent decrease in the proton paramagnetic relaxation rate during the transmetallation process. A 'long time index' equal to the ratio of the paramagnetic relaxation rate after 4320 min $[R_1^p(4320)]$ and its initial value $[R_1^p(0)]$ and a 'ratio index' set as the time (t) required to reach a ratio $R_1^p(t)/R_1^p(0) = 80\%$ were defined. As observed previously for open-chain complexes (31), the bisamide compound **3** shows faster and more extensive transmetallation than its parent complex Magnevist (**1**). In contrast, the C-functionalised compound MultiHance (**5**) (Fig. 5 and Table 4) undergoes a slower and more limited transmetallation process than Magnevist (**1**). This behaviour had already been observed for several other backbone-substituted derivatives of Magnevist (17,23,31–33). Macrocyclic complexes **2** and **4** have already been shown to be remarkably stable during the whole observation period (31), with decomplexation less than 10% after 5000 min (3.5 days). The data obtained in this work with Gadovist (**6**) confirm the previous results.

Interaction with HSA

The interaction of the gadolinium complex with HSA increases its rotational correlation time and subsequently enhances its paramagnetic relaxation rate. The resulting relaxivity increase depends on the relative amounts of free and bound contrast agents, and therefore on the strength of the interaction and on the intensity of the magnetic field. The proton NMRD profiles of the paramagnetic relaxation rate of solutions containing 1 mM of the contrast agents and 4% of HSA are shown in Fig. 6. For Magnevist (**1**), Dotarem (**2**), Omniscan (**3**), ProHance (**4**) and Gadovist (**6**) the curves are similar to their corresponding NMRD profiles in water, but a significant difference is observed for Multihance (**5**), which is known to interact with plasma proteins (34,35). The presence of HSA also induces a viscosity increase (0.87 mPa s compared with 0.69 mPa s at 310 K), which should result

Table 3. Proton relaxivity at 0.47 and 1.41 T and values of τ_M, τ_R, τ_{SO} and τ_V obtained from the proton NMRD profiles

	r_1^{310} (s^{-1} mM^{-1})						
Complex	$B_0 = 0.47$ T	$B_0 = 1.41$ T	τ_M^{310} (ns)	τ_R^{310} (ps)	τ_{S0}^{310} (ps)	τ_V^{310} (ps)	r^a (nm)
Magnevist (**1**)	3.8	3.4	143 ± 25	54 ± 1.4	87 ± 3	25 ± 3	0.31
Dotarem (**2**)	3.5	3.1	122 ± 10	53 ± 1.3	404 ± 24	7 ± 1	0.31
Omniscan (**3**)	3.8	3.6	967 ± 36	65 ± 2	95 ± 3	18 ± 3	0.31
Prohance (**4**)	3.6	3.2	217 ± 13	51 ± 2	142 ± 10	7.5 ± 2	0.31
MultiHance (**5**)	4.8	4.1	140 ± 11	89 ± 1.5	102 ± 2	30 ± 1	0.31
			140 ± 11	72 ± 1.3	88 ± 2	25 ± 1	0.30
Gadovist (**6**)	3.7	3.2	176 ± 21	57 ± 2	111 ± 6	6.5 ± 2	0.31

[a]Fixed parameter.

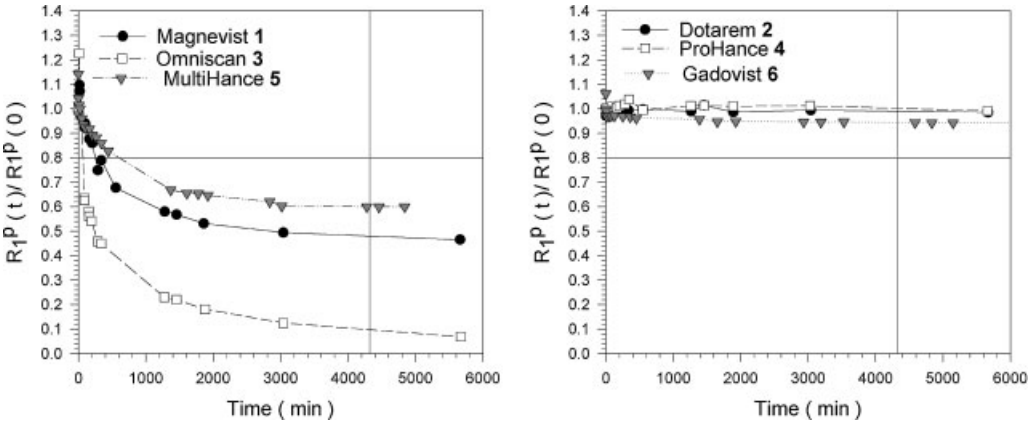

Figure 5. Evolution of $R_1^p(t)/R_1^p(0)$ versus time for Magnevist (**1**), Omniscan (**3**) and MultiHance (**5**) (left-hand graph) and Dotarem (**2**), ProHance (**3**) and Gadovist (**6**) (right-hand graph). Initial concentrations of Gd complexes and $ZnCl_2$ are 2.5 mM in phosphate buffer (pH 7), $T = 310$ K, $B = 0.47$ T. The vertical line corresponds to time = 4320 min, the horizontal line corresponds to an $R_1^p(t)/R_1^p(0)$ value of 0.8.

in increased values of τ_R and decreased values of the relative diffusion constant D. Theoretical fittings performed with the parameters of the free Gd complexes but taking into account these viscosity effects on τ_R and D are shown in Fig. 6 together with the fitting of the data obtained in water. For complexes **1**, **2**, **3**, **4** and **6**, the experimental data are close to the fitted profiles at all magnetic fields, indicating that the presence of HSA does not significantly modify the physicochemical parameters of the complexes. In contrast, the differences between the theoretical profiles of Gd–BOPTA and the experimental data are much larger over the whole magnetic field range, in agreement with the known interaction with HSA.

The analysis of the paramagnetic proton relaxation rate of solutions containing 4% of HSA and increasing amounts of MultiHance (Fig. 7) allows the evaluation of the association constant and of the relaxivity of the bound complex at 0.47 T. These were found to be equal to $2060 \pm 1290\ \text{M}^{-1}$ and $32.0 \pm 6.6\ \text{s}^{-1}\,\text{mM}^{-1}$, respectively [see Eqn. (1) in Materials and Methods]. It should be noted that the presence of 150 mM of NaCl markedly decreases the binding of MultiHance to HSA ($R_1^p = 8.33\ \text{s}^{-1}$ in the presence of salt compared with $13.8\ \text{s}^{-1}$ in the absence of salt for solutions containing 1 mM of MultiHance and 4% of HSA at 20 MHz and 310 K). In agreement with these results, Port et al. recently reported a lower value of the binding constant of Multihance in rabbit plasma ($K = 490\ \text{M}^{-1}$) and a slightly larger value of the relaxivity of the bound complex ($r_1^c = 36\ \text{s}^{-1}\,\text{mM}^{-1}$) (36). As stated by these authors, the interaction with HSA results in a concentration-dependent apparent relaxivity of MultiHance in HSA solution, with larger relaxivities at lower concentrations (Fig. 7).

The behaviour of MultiHance in the presence of HSA is similar to that of Primovist, another hepatobiliary derivative of Gd–DTPA substituted on the carbon backbone (16).

The amounts of free and bound complexes in the solution used for the NMRD measurements calculated using this K value are 65 and 35%, respectively. The proton NMRD profile calculated for the bound complex is shown in Fig. 8. The fitting of this curve was performed using the classical inner-sphere (27,28) and outer-sphere (29) models and also an additional contribution due to second-sphere water molecules (37). Some parameters were fixed: the number of water molecules coordinated to the Gd^{3+} ion ($q = 1$); the distance between the proton nuclei of the inner-sphere water molecule and Gd^{3+} ($r = 0.3$ nm); the relative diffusion constant ($D = 2.9 \times 10^{-9}\ \text{m}^2\,\text{s}^{-1}$) (26); the distance of closest

Table 4. Long time and ratio indexes of the zinc(II) transmetallation process

Complex	Long time index[a]	Ratio index[b] (min)
Magnevist (**1**)	0.49	250
Dotarem (**2**)	0.99	>5000
Omniscan (**3**)	0.10	70
ProHance (**4**)	0.99	>5000
MultiHance (**5**)	0.60	600
Gadovist (**6**)	0.95	>5000

[a] $R_1^p(t = 4320\ \text{min})/R_1^p(t = 0\ \text{min})$.
[b] Time required for $R_1^p(t)/R_1^p(t = 0\ \text{min}) = 0.8$.

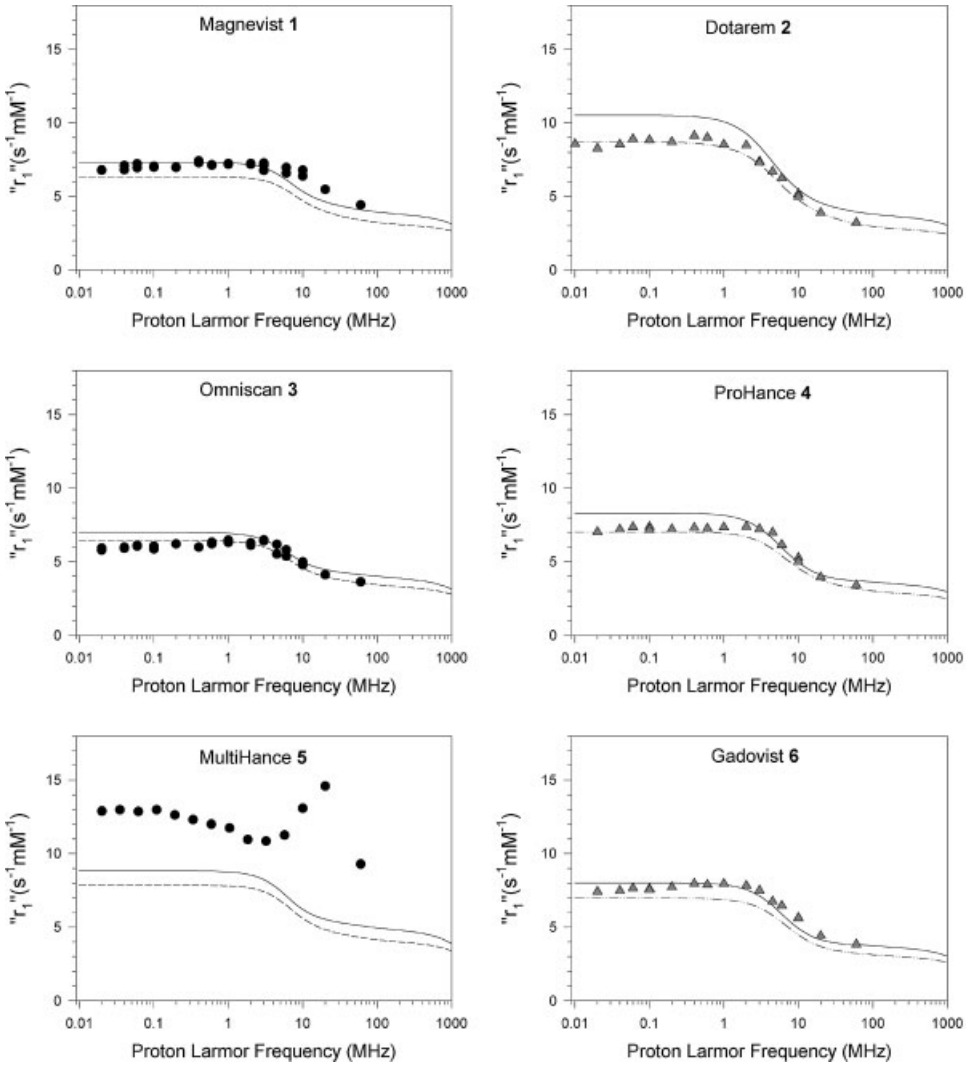

Figure 6. Apparent relaxivity profiles of solutions containing 1 mM of the contrast agents and 4% of HSA. The lower dashed lines correspond to the theoretical fittings obtained in water and the upper solid lines correspond to the expected profiles when the effects of the viscosity increase on τ_R and D are taken into account.

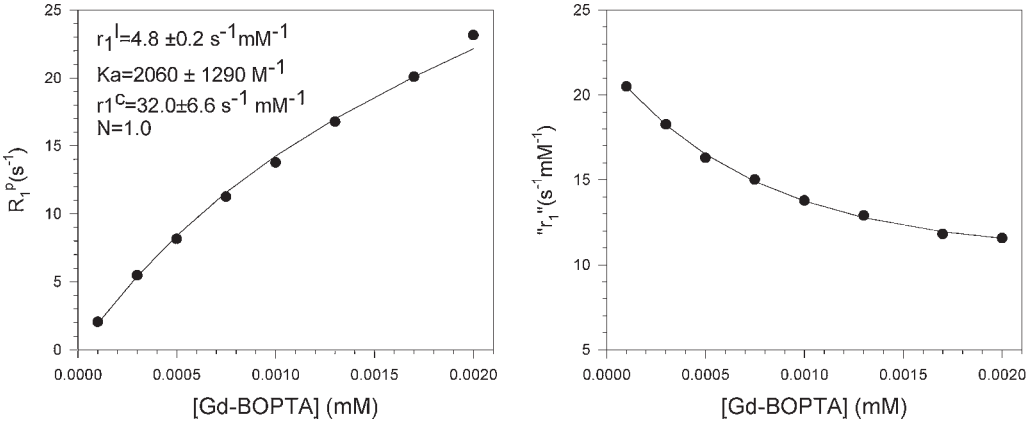

Figure 7. Paramagnetic proton relaxation rate (left) and apparent relaxivity (right) of solutions containing 4% of HSA and increasing concentrations of MultiHance (**5**) at 20 MHz and 310 K.

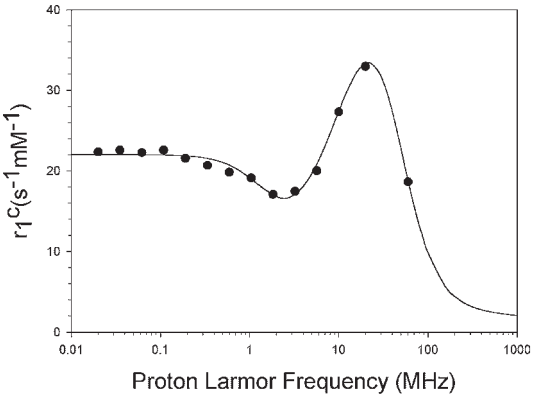

Figure 8. Calculated proton NMRD profile of MultiHance (**5**) bound to HSA at 310 K.

approach for the outer sphere contribution ($d = 0.45$ nm); and the distance between the atoms of the second-sphere water molecules ($r_{SS} = 0.4$ nm). τ_R, τ_M, τ_{SS} (the correlation time modulating the second-sphere contribution), q_{SS} (the number of water molecules in the second sphere), τ_V and τ_{SO} were optimised for the three contributions simultaneously. Satisfactory fit of the data could be obtained with the following values: $\tau_R = 11.8 \pm 0.9$ ns, $\tau_M = 450 \pm 14$ ns, $\tau_{SO} = 207 \pm 12$ ps, $\tau_V = 38.8 \pm 1$ ps, $\tau_{SS} = 43.1 \pm 4.4$ ps and $q_{SS} = 4.2 \pm 0.3$ (Fig. 8). The τ_R value agrees with a markedly reduced mobility of the contrast agent bound to the protein.

The interaction has also been evidenced by electrospray ionisation mass spectrometry, through the occurrence of peaks corresponding to the HSA–MultiHance complex (38).

CONCLUSIONS

As expected, depending on their structure and size, the rotational correlation times at 310 K range from 53 to 72 ps for the open-chain complexes and from 51 to 53 ps for the macrocyclic complexes. Their τ_{SO} values range between 87 and 142 ps, except for Dotarem (2), which is characterized by a larger value. The τ_V values of linear complexes seem to be larger than those of macrocyclic complexes. Regarding the water exchange rate, the bisamide derivative Omniscan is clearly different, with a τ_M value close to 1 μs at 310 K, whereas the τ_M of all other complexes ranges between 120 and 220 ns. Complexes **1**, **2**, **3**, **4** and **6** have similar relaxivity in the imaging field region whereas MultiHance **(5)** is slightly more efficient. The transmetallation process by zinc(II) ions at pH 7 in phosphate buffer is negligible for all macrocyclic complexes. Among the open-chain complexes, MultiHance (**5**) seems to be more stable than the parent complex **1**. Additionally, only MultiHance interacts with HSA, resulting in a higher apparent relaxivity varying from 20.5 s^{-1} mM^{-1} for a concentration of 0.1 mM to 11.6 s^{-1} mM^{-1} for a concentration of 2 mM at 20 MHz and 310 K in 0.6 mM HSA solution.

In the context of molecular imaging, bisamide derivatives of open-chain and macrocyclic complexes should be avoided because of their slow water exchange and, hence, the quenching of their efficacy. In contrast, tracers based on the Magnevist **(1)** structure but substituted on the carbon backbone would be preferable because of the cumulative effects of their enhanced proton relaxivity, their relatively fast water exchange and their increased stability versus zinc(II) transmetallation. Macrocyclic derivatives are also well suited for these applications owing to their very high stability in physiological media and their relatively fast water exchange rate.

MATERIALS AND METHODS

Chemicals

Measurements were performed on the available clinical formulations of the various contrast agents.

Oxygen-17 NMR

^{17}O NMR measurements of solutions were performed at 7.05 T on 2-mL samples contained in 10 mm o.d. tubes on a Bruker AMX-300 spectrometer (Bruker, Karlsruhe, Germany). Temperature was regulated by air or nitrogen flow controlled by a Bruker BVT 2000 unit. ^{17}O transverse relaxation times of distilled water (pH 6.5–7) were measured using a CPMG sequence and a subsequent two-parameter fit of the data points. The 90° and 180° pulse lengths were 25 and 50 μs, respectively. The ^{17}O T_2 of water in complex solution was obtained from linewidth measurements. All spectra were proton decoupled. The concentration of the samples was lower than 25 mM. The data are presented as the reduced transverse relaxation rate $\{1/T_2^R = 55.55/([\text{Gd complex}]qT_2^p)$, where [Gd complex] is the molar concentration of the complex, q is the number of coordinated water molecules and T_2^p is the paramagnetic transverse relaxation rate$\}$. The treatment of the experimental data was performed as already described (16–18).

Proton NMRD

Proton nuclear magnetic relaxation dispersion (NMRD) profiles were measured on a Stelar Spinmaster FFC fast field cycling NMR relaxometer [Stelar, Mede (PV), Italy] over a magnetic field strength range extending from 0.24 mT to 0.24 T or on a field cycling relaxometer (Field Cycling Systems, Honesdale, PA, USA) over a magnetic

field range from 0.24 mT to 1.0 T. Measurements were performed on 0.6-mL samples contained in 10 mm o.d. Pyrex tubes. Additional relaxation rates at 20, 60 and 300 MHz were obtained on a Minispec PC-120, a Minispec mq60 and a Bruker AMX-300 spectrometer, respectively. Proton NMRD curves were fitted using data-processing software (39,40) including different theoretical models describing nuclear relaxation phenomena (Minuit, CERN Library) (27–29).

Transmetallation kinetics

The technique is based on the measurement of the evolution of the water proton paramagnetic longitudinal relaxation rate (R_1^p) of a buffered solution ($[KH_2PO_4] = 0.026\,mol\,L^{-1}$, $[Na_2HPO_4] = 0.041\,mol\,L^{-1}$, pH 7) containing 2.5 mM gadolinium complex and 2.5 mM $ZnCl_2$(31). The measurements were performed on a Minispec PC-120 spin analyser (Bruker) at 20 MHz and 310 K. The samples (0.3 mL) were contained in 7 mm o.d. Pyrex tubes and were kept at 310 K in a dry block between measurements (up to 4 days).

HSA interaction

The analysis of the paramagnetic relaxation rates in HSA solutions (R_1^{pobs}) containing increasing amounts of Gd complexes at 20 MHz and 310 K was performed using the equation

$$R_1^{p^{obs}} = 1000 \times [(r_1^f \times s^0) + \tfrac{1}{2}(r_1^c - r_1^f) \times \{(N \times p^0) + s^0 + K^{-1} - \sqrt{[(N \times p^0) + s^0 + K^{-1}]^2 - 4 \times N \times s^0 \times p^0}\}] \quad (1)$$

where p^0 and s^0 are the initial concentrations of protein and contrast agent respectively, r_1^c and r_1^f are the relaxivity of the bound and free complexes, N is the number of identical binding sites and K their association constant. N was set to 1.

Acknowledgements

This work was supported by the FNRS and the ARC Program 00/05-258 of the French Community of Belgium. The support and sponsorship concerted by COST Action D18 'Lanthanide Chemistry for Diagnosis and Therapy' and the EMIL Network of Excellence of the 6th Framework Program of the European Community are gratefully acknowledged.

REFERENCES

1. Lauffer R. Paramagnetic metal complexes as water proton relaxation agents for MRI: theory and design. *Chem. Rev.* 1988; **87**: 901–927.
2. Caravan P, Ellison JJ, McMurry TJ, Lauffer R. Gadolinium(III) chelates as MRI contrast agents: structure, dynamics and applications. *Chem. Rev.* 1999; **99**: 2293–2352.
3. Weinmann H-J, Brasch RC, Press W-R, Wesbey GE. Characteristics of gadolinium–DTPA complex, a potential NMR contrast agent. *Am. J. Roentgenol*. 1984; **142**: 619–624.
4. Caillé JM, Bonnemain B, Allard M, Kien P. Gadolinium–DOTA in preclinical applications. In *Contrast and Contrast Agents in Magnetic Resonance Imaging. A Special Topic Seminar*, Rinck PA (ed.). European Workshop on Magnetic Resonance in Medicine Dpt of General, Organic and Biomedical, NMR and Molecular Imaging Laboratory, 7000 Mons, Belgium. Trondheim; 1988; 44–64.
5. Magerstadt M, Gansow OA, Brechbiel MW, Colcher D, Baltzer L, Knop RH, Girton ME, Naegele M. Gadolinium–(DOTA): an alternative to gadolinium–(DTPA) as a *T*1,2 relaxation agent for NMR imaging or spectroscopy. *Magn. Reson. Med*. 1986; **3**: 808–812.
6. Bousquet JC, Saini S, Stark DD, Hahn PF, Nigam M, Wittenberg J, Ferrucci JT. Gd–DOTA: characterisation of a new paramagnetic complex. *Radiology* 1988; **166**: 693–698.
7. Cacheris WP, Quay SC, Rocklage SM. The relationship between thermodynamics and toxicity of gadolinium complexes. *Magn. Reson. Imaging*. 1990; **8**: 467–481.
8. Zoarski GH, Lufkin RB, Bradley WG Jr, Flanders AE, Gale DR, Harms SE, Haughton VM, Joy SE, Kanal E, Rosa L. Multicenter trial of Gadoteridol, a nonionic gadolinium chelate, in patients with suspected head and neck pathology. *Am. J. Neuroradiol*. 1993; **14**: 955–961.
9. Tombach B, Heindel W. Value of 1.0-M gadolinium chelates: review of preclinical and clinical data on gadobutrol. *Eur. Radiol*. 2002; **12**: 1550–1556.
10. Vogler H, Platzek J, Schuhmann-Giampieri G, Frenzel T, Weimann H-J, Radüchel B, Press W-R. Pre-clinical evaluation of gadobutrol: a new neutral, extracellular contrast agent for magnetic resonance imaging. *Eur. J. Radiol*. 1995; **21**: 1–10.
11. Platzek J, Blaszkiewicz P, Gries H, Luger P, Mishl G, Muller-Fahrnow A, Raduchel B, Sulzle D. Synthesis and structure of a new macrocyclic polyhydroxylated gadolinium chelate used as a contrast agent for magnetic resonance imaging. *Inorg. Chem*. 1997; **36**: 6086–6093.
12. Uggeri F, Aime S, Anelli PL, Botta M, Brocchetta M, de Haen C, Ermondi G, Grandi M, Paoli P. Novel contrast agents for magnetic resonance imaging. Synthesis and characterisation of the ligand BOPTA and its Ln(III) complexes (Ln = Gd, La, Ln). X-ray structure of disodium (TPS-9-145337286-C-S)-[4-carboxy-5,8,11-tris(carboxymethyl)-1-phenyl-2-oxa–5,8,11-triazatridecan-13-oato(5−)] gadolinite (2−) in a mixture with its enantiomer. *Inorg. Chem*. 1995; **34**: 633–642.
13. Tweedle MF, Hagan JJ, Kumar K, Mantha S, Chang CA. Reaction of gadolinium chelates with endogenously available ions. *Magn. Reson. Imaging* 1991; **9**: 409–415.
14. Wedeking P, Kumar K, Tweedle MF. Dissociation of gadolinium chelates in mice: relationship to chemical characteristics. *Magn. Reson. Imaging* 1992; **10**: 641–648.
15. Tweedle MF, Wedeking P, Kumar K. Biodistribution of radiolabeled, formulated gadopentetate, gadoteridol, gadoterate and gadodiamide in mice and rats. Invest. *Radiol*. 1995; **30**: 372–380.
16. Vander Elst L, Maton F, Laurent S, Seghi F, Chapelle F, Muller RN. A multinuclear MR study of Gd–EOB–DTPA: comprehensive preclinical characterisation of an organ specific MRI contrast agent. *Magn. Reson. Med*. 1997; **38**: 604–614.
17. Muller RN, Raduchel B, Laurent S, Platzek J, Pierart C, Mareski P, Vander Elst L. Physicochemical characterisation of MS-325, a new gadolinium complex, by multinuclear relaxometry. *Eur. J. Inorg. Chem*. 1999; 1949–1955.
18. Laurent S, Vander Elst L, Houze S, Guerit N, Muller RN. Synthesis and characterisation of various benzyl diethylenetriaminepentaacetic acids (dtpa) and their paramagnetic complexes. Potential

contrast agents for magnetic resonance imaging. *Helv. Chim. Acta* 2000; **83**: 394–406.
19. Botteman F, Nicolle GM, Vander Elst L, Laurent S, Merbach AE, Muller RN. Synthesis, variable temperature and pressure O-17 NMR study of bis(alkylamide) derivatives of (Gd–DTPA)(H_2O)](2−)—An assessment of the substitution effect on water exchange kinetics. *Eur. J. Inorg. Chem*. 2002; 2686–2693.
20. Micskei K, Helm L, Brucher E, Merbach AE. ^{17}O NMR study of water exchange on $[Gd(DTPA)H_2O]^{2-}$ and $[Gd(DOTA)H_2O]^{-}$ related to NMR imaging. *Inorg. Chem*. 1993; **32**: 3844–3850.
21. Gonzalez G, Powell DH, Tissières V, Merbach AE. Water-exchange, electronic relaxation and rotational dynamics of the MRI contrast agent [Gd(DTPA–BMA)(H_2O)] in aqueous solution: a variable pressure, temperature and magnetic field ^{17}O NMR study. *J. Phys. Chem*. 1994; **98**: 53–59.
22. Powell DH, Ni Dhubhghaill OM, Pubanz D, Helm L, Lebedev YS, Schlaepfer W, Merbach AE. Structural and dynamic parameters obtained from ^{17}O NMR, EPR and NMRD studies of monomeric and dimeric Gd^{3+} complexes of interest in magnetic resonance imaging: an integrated and theoretically self-consistent approach. *J. Am. Chem. Soc*. 1996; **118**: 9333–9346.
23. Laurent S, Botteman F, Vander Elst L, Muller RN. New bifunctional contrast agents: bis-amide derivatives of C-substituted Gd–DTPA. *Eur. J. Inorg. Chem*. 2004; 463–468.
24. Botteman F. Synthesis and characterisation of Ln-DTPA like complexes. Influence of the structure on the dynamics of exchange of the coordinated water, PhD Thesis, University of Mons-Hainaut, Belgium 2002.
25. Vander Elst L, Laurent S, Muller RN. Multinuclear MR characterisation of paramagnetic contrast agents: the manifold effects of concentration. *Invest. Radiol*. 1998; **33**: 828–834.
26. Vander Elst L, Sessoye A, Laurent S, Muller RN. Is the theoretical fitting of the proton nuclear magnetic relaxation dispersion (NMRD) curves of paramagnetic complexes improved by independent measurement of their self-diffusion coefficients? *Helv. Chim. Acta* 2005; **88**: 574–587.
27. Solomon I. Relaxation processes in a system of two spins. *Phys. Rev.* 1955; **99**: 559–565.
28. Bloembergen N. Proton relaxation times in paramagnetic solutions *J. Chem. Phys*. 1957; **27**: 572–573.
29. Freed JH. Dynamic effects of pair correlation functions on spin relaxation by translational diffusion in liquids. II. Finite jumps and independent T_1 processes. *J. Chem. Phys*. 1978; **68**: 4034–4037.
30. Caravan P, Astahkin AV, Raitsimring AM. The gadolinium(III)–water hydrogen distance in MRI contrast agents. *Inorg. Chem*. 2003; **42**: 3972–3974.
31. Laurent S, Vander Elst L, Copoix F, Muller RN. Stability of MRI paramagnetic contrast media. A proton relaxometric protocol for transmetallation assessment. *Invest. Radiol*. 2001; **36**: 115–122.
32. Laurent S, Botteman F, Vander Elst L, Muller RN. Optimising the design of paramagnetic MRI contrast agents: influence of backbone substitution on the water exchange rate of DTPA derivatives. *Magn. Reson. Mater. Phys. Biol. Med. (MAGMA)* 2004; **16**: 235–245.
33. Laurent S, Botteman F, Vander Elst L, Muller RN. Relaxivity and stability of new C-4 benzyl derivatives of Gd–DTPA. Helv. *Chim. Acta* 2004; **87**: 1077–1089.
34. Cavagna FM, Marzola P, Dapra M, Maggioni F, Vicinanza E, Castelli PM, de Haen C, Luchinat C, Wendland MF, Saeed M, Higgins CB. Binding of gadobenate dimeglumine to proteins extravasated into interstitial space enhances conspicuity of reperfused infarcts. Invest. *Radiol*. 1994; **29**: S50–S53.
35. Cavagna FM, Maggioni F, Castelli PM, Dapra M, Imperatori LG, Lorusso V, Jenkins BG. Gadolinium chelates with weak binding to serum proteins. A new class of high-efficiency, general purpose contrast agents for magnetic resonance imaging. *Invest. Radiol*. 1997; **32**: 780–796.
36. Port M, Corot C, Violas X, Robert Ph, Raynal I, Gagneur G. How to compare the efficiency of albumin-bound and nonalbumin-bound contrast agents *in vivo*. The concept of dynamic relaxivity. *Invest. Radiol*. 2005; **40**: 565–573.
37. Aime S, Botta M, Fedeli F, Gianolio E, Terreno E, Anelli P. High-relaxivity contrast agents for magnetic resonance imaging based on multisite interactions between a β-cyclodextrin oligomer and suitably functionalized GdIII chelates. *Chem. Eur. J*. 2001; **7**: 5262–5269.
38. Henrotte V. Unpublished results.
39. Muller RN, Declercq D, Vallet P, Giberto F, Daminet B, Fischer HW, Maton F, Van Haverbeke Y. In *Proceedings of ESMRMB, 7th Annual Congress*, Strasbourg, 1990, p. 394.
40. Vallet P. Relaxivity of nitroxide stable free radicals. Evaluations by field cycling method and optimisation, PhD Thesis, University of Mons-Hainaut, Belgium, 1992.

